Modelling and Control of Conjugated Polymer Actuators Using Robust Control QFT

Keivan Torabi Z.[1], Majid Moavenian[2], Amir Ali Amiri Moghadam[3] Amir Hossein Amiri Moghadam[4]

[1]Assistant Professor, University of Kashan; kvntrb@kashanu.ac.ir
[2] Assistant Professor, Ferdowsi University of Mashhad; moaven@um.ac.ir
[3]PhD student, Ferdowsi University of Mashhad; am_am302@stu-mail.um.ac.ir
[4]Mechanical Engineer Supervisor, Mashhad urban railway; amirhosein121@gmail.com

Abstract
Conjugated polymer actuators can be employed to achieve micro and nano scale precision, and have wide range of application including biomimetic robots, and biomedical devices. In comparison to robotic joints, they do not have friction or backlash, but on the other hand, they have complicated electro-chemo-mechanical dynamics which makes accurate and robust control of the actuator really difficult. This paper consists of two major parts. In the first part the infinite-dimensional physical model of actuator will be replaced with a family of linear uncertain transfer functions based on Golubev Method. Further model development will take into account the influence of reduction/oxidation level on the variation of the actuator resistance and the evaporation of the solvent. In the second part the robust control QFT will be applied to control the highly uncertain dynamics of the conjugated polymer actuators. The main steps involved in the design of a QFT controller are template generation, loop shaping, and pre-filter design. Finally the analysis of design shows that QFT controller has consistent and robust tracking performance.

Keywords: Conjugated polymer actuators, Polypyrrole, Uncertainty, QFT.

Introduction

There is an increasing request for new generation of actuators which can be used in devices such as artificial organs, micro robots, human-like robots, and medical applications. Up to now lots of research has been done on developing new actuators such as shape memory alloys, piezoelectric actuators, magnetostrictive actuators, contractile polymer actuators, and electrostatic actuators [1], [2]. The main disadvantages of these actuators are low efficiency, high electrical power, and low strain generation [2]. Conjugated polymers actuators seams to be the best solution since they produce reasonable strain under low input voltage.
The main process which is responsible for volumetric change and the resulted actuation ability of the conjugated polymer actuators is Reduction/Oxidation (RedOx).Thus based on different fabrication form, different configuration of the actuators can be obtained namely: linear extenders, bilayer benders, and trilayer benders [3-5]. By applying a voltage to the actuator, the polypyrrole (PPy) layer on the anode side is oxidized while that on the cathode side is reduced. Ions can transfer inside the Conjugated Polymer Actuators based on two main mechanisms namely diffusion and drift [6]. The main objective of this paper is to synthesize suitable controller and pre-filter such that, first the closed loop system is stable, second it can track desired inputs. As mentioned before the uncertainty in the dynamics of actuators is inevitable, therefore application of robust control techniques is essential for achieving high precision. There are two basic methodologies for dealing with the effect of uncertainty in a system namely adaptive control and robust control. In adaptive control design approach, the controller will estimate the system's parameter online and then will tune itself based on these estimates. In the robust control design approach, the controller has a fixed structure which will satisfy the system specifications over whole range of plant uncertainty. Although adaptive control can be applied to a wider class of problems, the application of robust control will lead to a simpler controller as the structure of controller is fixed requiring no time for tuning [7].

I. Trilayer PPy actuator

In this paper as an example of the Conjugated polymer actuators the trilayer PPy actuator will be considered. Figure 1 depicts the trilayer PPy actuator. As the name indicates the trilayer PPy actuator consists of three layers. The middle layer is Porous Polyvinylidene Fluoride (PVDF) which is used as a storage tank for the electrolyte. And on the both sides of it there are polymer layers (PPy) [8], [9].

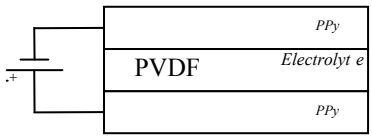

Figure 1: Three-layer PPy actuator

As it has mentioned before the main process which is responsible for volumetric change of the conjugated polymer actuators is RedOx. Thus in the trilayer bender while the PPy layer on the anode side is oxidized and expands as a result, the PPy layer on the cathode side is reduced and contracts as a result. Therefore this difference in the volume will leads to the bending of the actuator.

II. Electro-chemo-mechanical modeling

The electro-chemo-mechanical model is comprised of two parts, namely electrochemical model and electromechanical model.

A. Electrochemical Modeling

The electrochemical model relates the input voltage and chemical RedOx reaction inside the PPy actuators. In this part firstly the admittance model for a bilayer actuator will be achieved, and next this model will be extended to the trilayer PPy actuator. Figure 2 depicts

the electrical admittance model. Based on the Diffusive-Elastic-Metal model, transportation of ions within the polymer is only caused by diffusion [6].

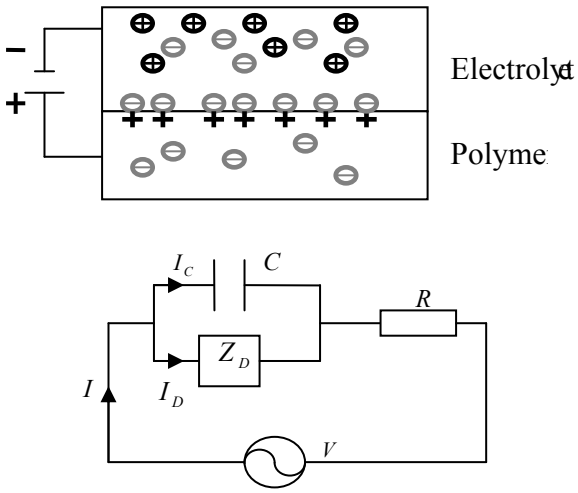

Figure 2: Description of diffusion and double layer charging and its equivalent electrical circuit

According to Figure 2 and the Kirchhoff's voltage law one has:

$$I(s) = I_c(s) + I_D(s) \tag{1}$$

$$V(s) = I(s).R + \frac{1}{s.C} I_C(s) \tag{2}$$

Where Z_D is the diffusion impedance, C denotes the double-layer capacitance, and R is the electrolyte and contact resistance. Next based on Figure 3 and the Fick's law of diffusion, diffusion current is:

$$i_D(t) = -F.A.D.\left.\frac{\partial c(x,t)}{\partial x}\right|_{x=0} \tag{3}$$

Where A is the surface area of the polymer, F is the Faraday constant, D is the diffusion coefficient, h is the thickness of the PPy layer, and c is the concentration ions.

The current of double-layer capacitance is

$$i_C(t) = F.A.\delta.\left.\frac{\partial c(x,t)}{\partial t}\right|_{x=0} \tag{4}$$

Where δ is the double-layer capacitance thickness. And the diffusion equation is

$$\frac{\partial c}{\partial t} = D\frac{\partial^2 c}{\partial x^2} \qquad 0 < x < h \tag{5}$$

Finally the boundary condition is

$$\left.\frac{\partial c(x,t)}{\partial x}\right|_{x=h} = 0 \tag{6}$$

Now based on Equations 1, 2, 3, 4, 5, and 6, it can be shown that the admittance model ($Y(s) = \frac{I(s)}{V(s)}$) of a conjugated polymer [6].

$$Y(s) = \frac{s\left[\frac{\sqrt{D}}{\delta}\tanh(h\sqrt{s/D}) + \sqrt{s}\right]}{\frac{\sqrt{s}}{C} + Rs^{3/2} + R\frac{\sqrt{D}}{\delta}s\tanh(h\sqrt{s/D})} \tag{7}$$

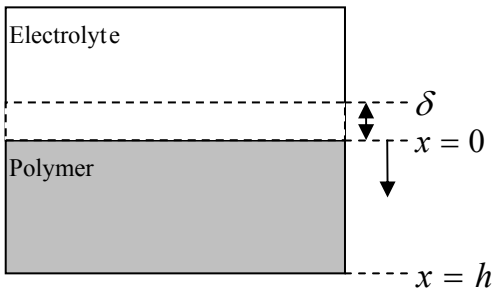

Figure 3: Description of frame assignment for diffusion

According to Figure 1 in the case of a trilayer bender the input voltage is applied across two double-layers, thus the admittance is half of Equation 7.

$$Y(s)_{tri} = \frac{1}{2}.\frac{s\left[\frac{\sqrt{D}}{\delta}\tanh(h\sqrt{s/D}) + \sqrt{s}\right]}{\frac{\sqrt{s}}{C} + Rs^{3/2} + R\frac{\sqrt{D}}{\delta}s\tanh(h\sqrt{s/D})} \tag{8}$$

B. Electromechanical Modeling

The electromechanical model relates the input voltage and bending displacement of the PPy actuators. It was shown that the relation between the induced in-plane strain (ε) and the density of the transferred charges (ρ) is as below [10]:

$$\varepsilon = \alpha.\rho \tag{9}$$

Where α is the strain-to-charge ratio. Thus, the induced stress is

$$\sigma = \alpha.E_{PPy}.\rho \tag{10}$$

Where E_{PPy} is the Young's modulus of PPy, and ρ can be achieved In the Laplace domain as below [11]:

$$\rho(s) = \frac{I(s)}{s\,W\,L\,h} \tag{11}$$

Where W is the width of the PPy, and L is the length of the PPy.

According to Figure 4 the curvature λ under the induced stress and in the absence of external force is [11].

$$\lambda = \frac{3\alpha}{2h_{pvdf}}.\frac{\left(1+\frac{h}{h_{pvdf}}\right)^2 - 1}{\left(1+\frac{h}{h_{pvdf}}\right)^3 + \frac{E_{pvdf}}{E_{PPy}} - 1}.\rho \tag{12}$$

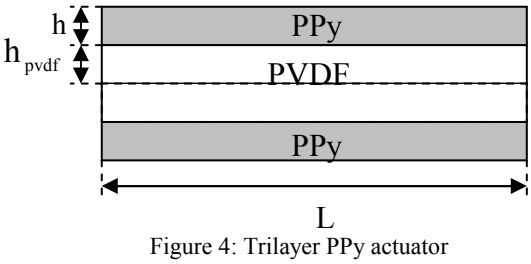

Figure 4: Trilayer PPy actuator

Where E_{pvdf} and h_{pvdf} are the Young's modulus and the thickness of the PVDF layer respectively.

According to Figure 5 one can obtain the relation between the bending displacement and the curvature as below:

$$r^2 = (r-y)^2 + L^2 \Rightarrow \lambda = \frac{1}{y} = \frac{2y}{y^2 + L^2}$$

By assuming that the bending displacement is small we have

$$\lambda = \frac{2y}{L^2} \tag{13}$$

Where y is the bending displacement.

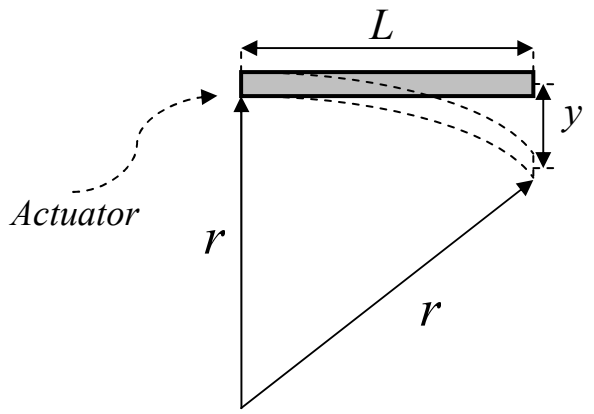

Figure 5: Relation between the bending displacement and the curvature

Finally by combining Equations 8, 10, 11, 12, and 13 one can obtain the full model between input voltage (V) and output displacement (y) as below [6],[11]:

$$\frac{y(s)}{V(s)} = \frac{C_m}{sR + \dfrac{1}{C(1 + \dfrac{\sqrt{D}}{\delta\sqrt{s}}\tanh(h\sqrt{\dfrac{s}{D}}))}} \tag{14}$$

Where

$$C_m = \frac{3\alpha L\left[\left(1 + \dfrac{h}{h_{pvdf}}\right)^2 - 1\right]}{8h_{pvdf}hW\left[\left(1 + \dfrac{h}{h_{pvdf}}\right)^3 + \dfrac{E_{pvdf}}{E_{ppy}} - 1\right]} \tag{15}$$

C. System identification based on Golubev Method

Because the term tanh in Equation 14 is not suitable for real time control of the actuator and this equation can not take into account the system uncertainties. In this part the Golubev Method [12] will be used to build a suitable model for control of the actuator. By replacing the term tanh with its equivalent series in Equation 14 the actuator model is [6]:

$$\frac{y(s)}{V(s)} = \frac{C_m}{sR + \dfrac{1}{C(1 + \dfrac{2D}{h\delta}\displaystyle\sum_{n=0}^{\infty}\frac{1}{s + \pi^2(2n+1)^2 D(2h)^{-2}})}} \tag{16}$$

In the first step one can study Equation 16 based on its summation term. For this purpose we use the typical values for physical parameters in Table 1[9].

Table 1: Values of physical parameters

Parameter	Value
D	$2\times10^{-10}\,m^2/s$
h	$30\,\mu m$
R	$15\,\Omega$
δ	$25\,nm$
C	$5.33\times10^{-5}\,F$

Thus based on Table 1and using different values for n (Number of terms in Equation 16) one can achieve Table 2.

Table 2: The actuator' system poles and zeros based on number of terms used.

No. of Terms	pole	zero
Two	-0.3793,- 3.848 ,- 2316	-2.736,-1069
Three	-0.3787,- 3.741 ,- 11.47, - 2854	-2.524,- 10.25 ,- 1606
Four	-0.378,- 3.696 ,- 11.19,- 23.5, - 3391	-2.432,- 9.778, - 22.29, - 2145

Based on Table 2 it can be seen that using two terms of Equation 16, will lead to a third order system. One zero and one pole of this system are located far to the left of the imaginary axis comparing to the other poles and zeros, thus the system can be reduced to a second order system. Similarly using three and four terms will lead to third and fourth order systems respectively. Therefore order of system depends on number of terms which is used. In order to solve this problem one can replace the infinite-dimensional system (using tanh) with a family of uncertain linear systems. Figure 6 compares the admittance of infinite-dimensional model with its estimation based on two, three, and four terms.

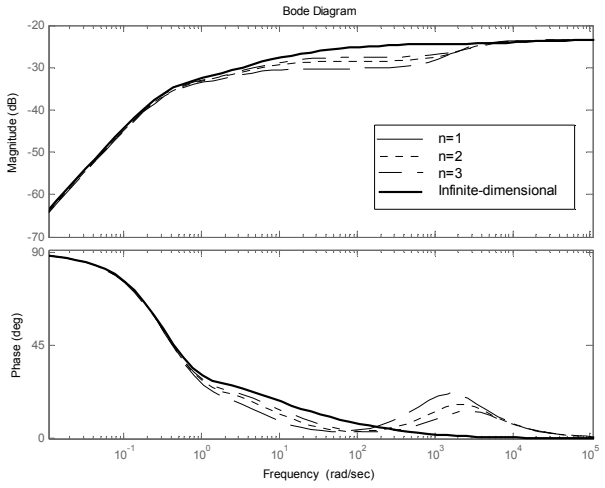

Figure 6: Comparisons between using different number of terms and the infinite-dimensional model

For example the parametric model for using three terms is as below:

$$\frac{y(s)}{V(s)} = \frac{a_1 s^3 + a_2 s^2 + a_1 s + a_4}{s^4 + b_1 s^3 + b_2 s^2 + b_3 s + b_4} \quad (17)$$

Where

$$Num(s) = \frac{C_m s^3}{R} + \left(\frac{6 C_m D}{\delta R h} + \frac{35}{4} \frac{C_m \pi^2 D}{R h^2} \right) s^2 + \left(\frac{35 C_m \pi^2 D^2}{\delta R h^3} + \frac{259}{16} \frac{C_m \pi^4 D^2}{R h^4} \right) s + \frac{259}{8} \frac{C_m \pi^4 D^3}{R \delta h^5} + \frac{225}{64} \frac{C_m \pi^6 D^3}{R h^6}$$

$$Den(s) = s^4 + \left(\frac{35}{4} \frac{\pi^2 D}{h^2} + \frac{6 D}{\delta h} + \frac{1}{RC} \right) s^3 + \left(\frac{35}{4} \frac{\pi^2 D}{R C h^2} + \frac{35 \pi^2 D^2}{\delta h^3} + \frac{259}{16} \frac{\pi^4 D^2}{h^4} \right) s^2 + \left(\frac{259}{16} \frac{\pi^4 D^2}{R C h^4} + \frac{259}{8} \frac{\pi^4 D^3}{\delta h^5} + \frac{225}{64} \frac{\pi^6 D^3}{h^6} \right) s + \frac{225}{64} \frac{\pi^6 D^3}{R C h^6}$$

First step in using the Golubev method is to simulate the actuator' model Figure 7, 8. Next by using Golubev method for different input signals (sin wave, step …), the uncertain transfer function is:

$$\frac{a_1 s^3 + a_2 s^2 + a_3 s}{s^3 + b_1 s^2 + b_2 s + b_3} \quad (18)$$

Where

$a_1 \in [0.05068, 0.06675]$; $a_2 \in [1.1, 1.211]$

$a_3 \in [2.3, 3.004]$; $b_1 \in [25.63, 26]$

$b_2 \in [95, 105]$; $b_3 \in [35, 45]$

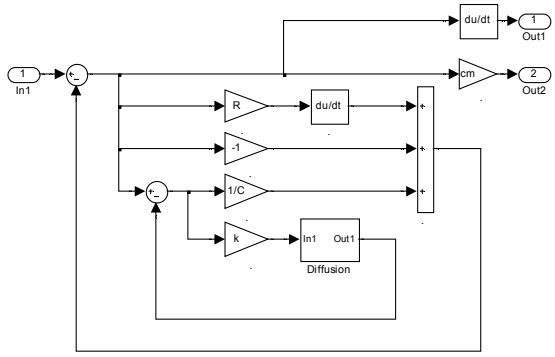

Figure 7: Simulation of the actuator model in Matlab

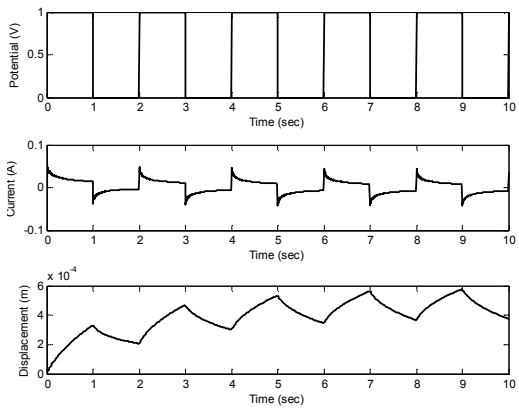

Figure 8: Voltage-current-displacement response of the actuator

Application of Golubev method for pulse signal is shown in Figure 9. Figure 10 depicts the admittance Bode plot of Equation 18.

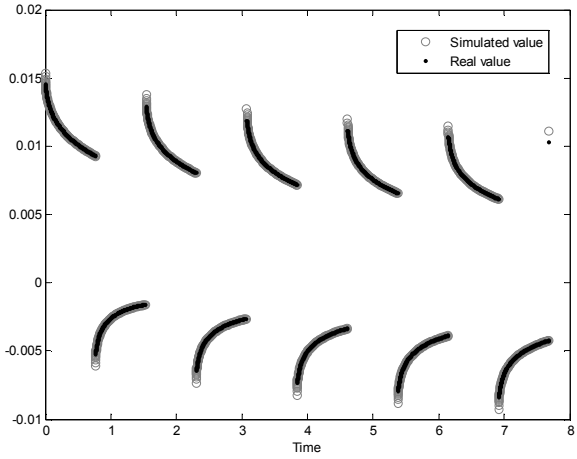

Figure 9: System identification based on pulse signal (Error=2.6973e-005)

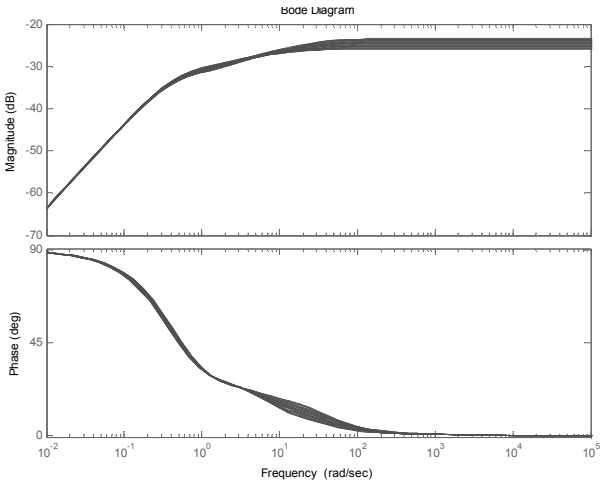

Figure 10: Admittance Bode plot based on Golubev method

In the next step the model will be developed further by considering the effect of actuator resistance and evaporation of the solvent. The actuator resistance is highly depends to the RedOx level [9, 13]. Figure 11 shows the Bode plot of actuator admittance for variation of resistance from $15\,\Omega$ to $100\,\Omega$. Variation of the diffusion coefficient is shown in Figure 12. Therefore by considering the above mentioned uncertainties the full uncertain model of the actuator is:

$$\frac{a_1 s^2 + a_2 s + a_3}{s^3 + b_1 s^2 + b_2 s + b_3} \quad (19)$$

Where

$a_1 \in [3.08 \times 10^{-4}, 0.001]$

$a_2 \in [0.0055, 0.0186]$

$a_3 \in [0.0154, 0.04634]$

$b_1 \in [25.63, 29]$

$b_2 \in [90, 105]$

$b_3 \in [20, 45]$

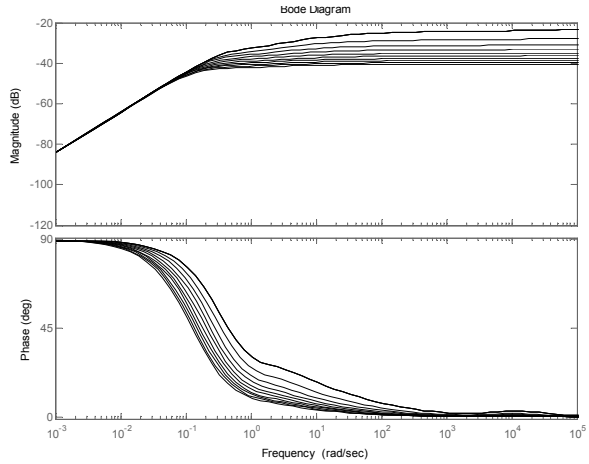

Figure 11 Bode plot of actuator admittance for variation of resistance

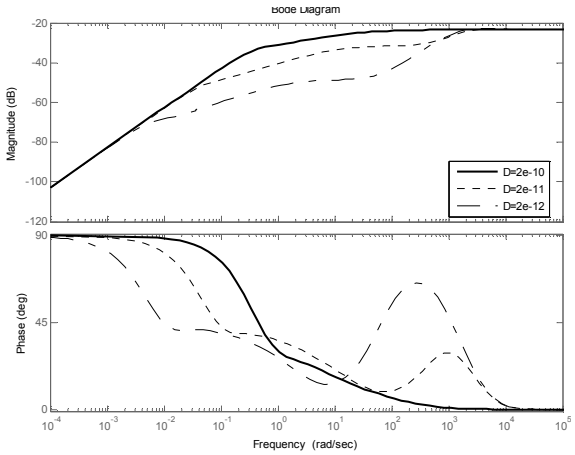

Figure 12: Bode plot of actuator admittance for variation of the diffusion coefficient

III. Application of QFT

There are many practical systems that have high uncertainty in open-loop transfer functions which makes it very difficult to have suitable stability margins and good performance in command following problems for the closed-loop system. Therefore a single fixed controller in such systems is found among "robust controllers" family.

Quantitative Feedback Theory (QFT) is a robust feedback control-system design technique initially introduced by Horowitz (1963, 1979), which allows direct design to closed-loop robust performance and stability specifications. Since then this technique has been developed by him and others [14], [15], [16], [17], and [18].

In many techniques from "robust control" family such as H_∞ design is based on magnitude of transfer function in frequency domain, but QFT is not only concerned with aforementioned subject, but also able to take into account phase information in the design process. The unique feature of QFT is that the performance specifications are expressed as bounds on frequency-response loop shapes in such a way that satisfaction of these bounds imply a corresponding approximate closed-loop satisfaction of some time-domain response bounds for given classes of inputs and for all uncertainty in a given compact set.

In parametric uncertain systems, we must first generate plant templates prior to the QFT design (at a fixed frequency, the plant's frequency response set is called a *template*). Given the plant templates, QFT converts closed loop magnitude specifications into magnitude constraints on a nominal open- loop function (these are called QFT *bounds*). A nominal open loop function is then designed to simultaneously satisfy its constraints as well as to achieve nominal closed loop stability. In a two degree-of-freedom design, a pre-filter will be designed after the loop is closed (i.e., after the controller has been designed) [19]. Figure 13 shows a two degree of freedom feedback system.

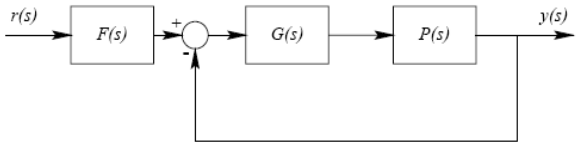

Figure 13Two degree of freedom feedback system

The objectives of this part are to synthesize suitable controller and pre-filter such that, first the closed loop system is stable, second it can track desired inputs. The robust margin is that the magnitude of closed loop system for all considered uncertainty must be less than 1.1. Robust tracking specification based on suitable performance of actuator is overshoot (=5%) and the settling time (=0.4s) for all plant uncertainty. At the first step we must define the plant uncertainty (template), which is shown in Figure 14. Then by having robust performance bounds in the loop-shaping phase of design suitable controller and Prefilter can be achieve as follows:

$$G = 2.1\times10^{7}\times \frac{(s+6.1)(s+0.48)(s+0.0098)}{(s+176.1)(s+0.5)(s+0.01)(s+1.4\times10^{-5})} \quad (3)$$

$$F = 0.011092\,\frac{(s^{2}+201s+2.02\times10^{4})}{(s+25.34)(s+8.841)} \quad (4)$$

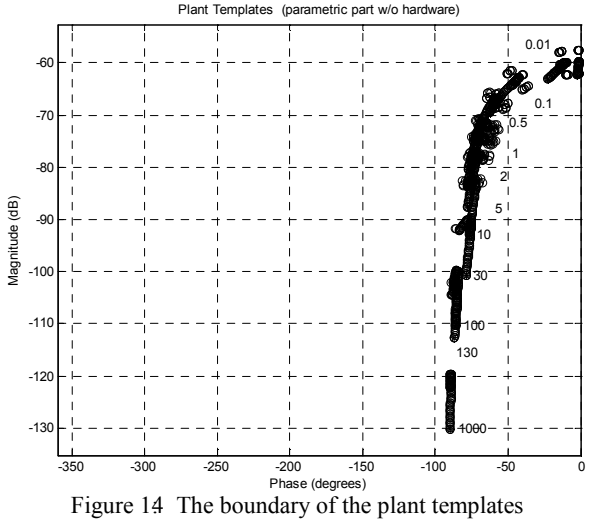

Figure 14 The boundary of the plant templates

Robust margin bounds are shown in Figure 15.Robust tracking bounds are shown in Figure 16.Figure 17 depicts the loop-shaping of open loop system. It can be observed that the nominal plant exactly lies on its performance bounds which confirm the optimality of design. Figure 18 shows time domain simulation for unit step responses.

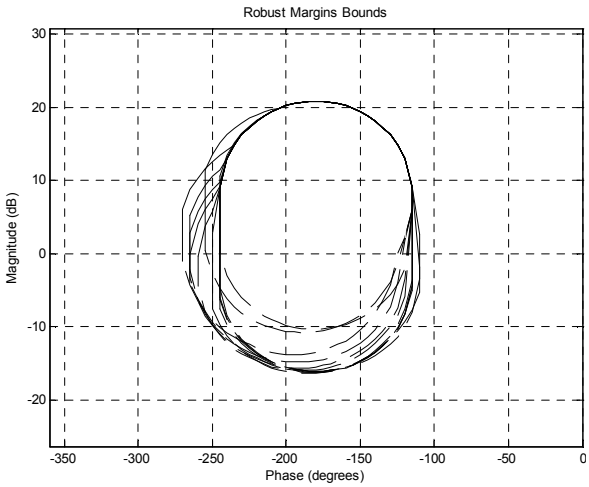

Figure 15: Robust margin

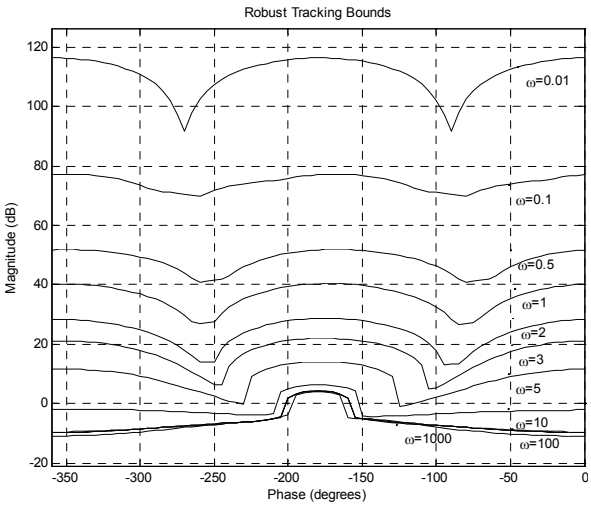

Figure 16: Robust tracking bounds

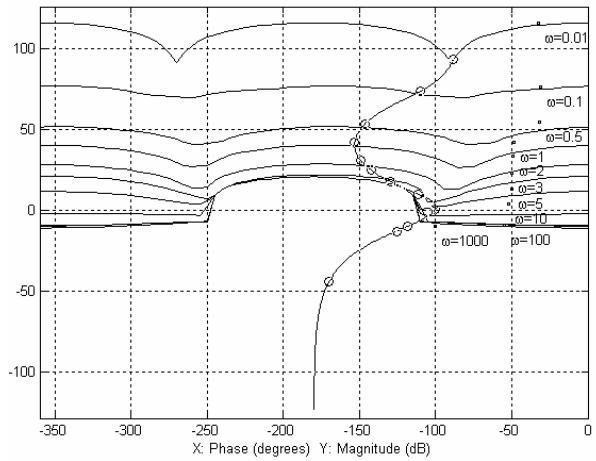

Figure 17: Loop shaping of open-loop system

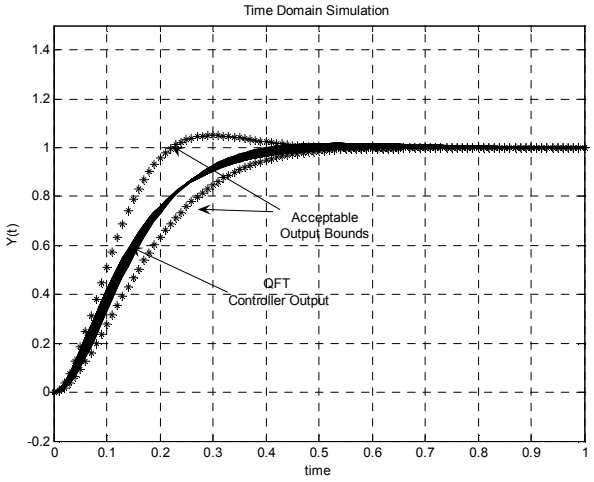

Figure 18: Unit step response for all considered uncertainty with acceptable output bounds

Figure 19 shows the tracking problem for the reference input $R = 0.5\times10^{-3}\sin(2\pi t)\ m$, while Figure 20 depicts the tracking error.

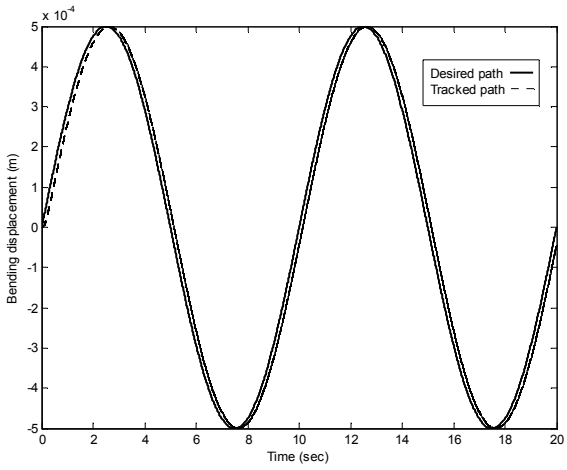

Figure 19: Tracking problem for a sin wave

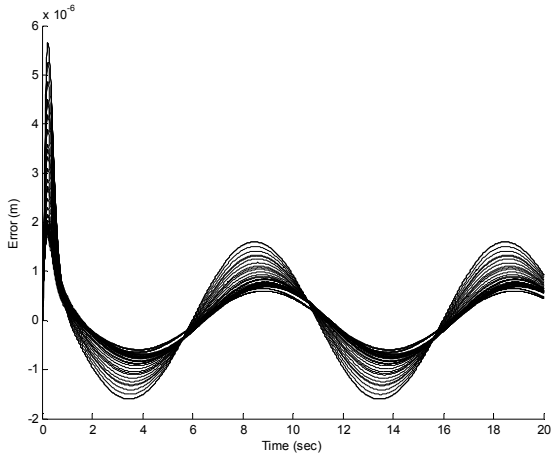

Figure 20Tracking error for all considered uncertainty

Resultsand Discussion

In this paper for the first time robust control QFT is applied to control the PPy actuators. In order to obtain a suitable model for controlling purposes, Golubev Method is used to convert the uncertain dynamics of

PPy actuators to a family of Linear Time Invariant systems.

Conclusions

By taking into the account the effects on uncertainties such as variation of the resistance and diffusion coefficient in the modeling part the J. Madden's model [6] improved greatly. In the controlling part it has been shown that the robust control QFT can successfully be applied to control the highly uncertain dynamics of PPy actuator. And also it has been shown that the actuator has robust tracking ability and robust stability under QFT controlling method.

References

[1]- Hollerbach, J.M., Hunter, I.W. and Ballantyne, J. *A comparative analysis of actuator technologies for robotics*. MIT press, 1999.

[2]- Ian W. Hunter and Serge Lafontaine, "A comparison of muscle with artificial actuators", Solid-State Sensor and Actuator Workshop, 5th Technical Digest, IEEE 1992.

[3] A. Della Santa, D. De Rossi, and A. Mazzoldi, "Characterization and modeling of a conducting polymer muscle-like linear actuator," Smart Materials and Structures, vol. 6, pp. 23–34, 1997.

[4] E. Smela, O. Inganas, and I. Lundstrom, "Controlled folding of microsize structures," Science, vol. 268, pp. 1735–1738, 1995.

[5] K. Kaneto, M. Kaneko, Y. Min, and A. G. MacDiarmid, "artificial muscle: Electromechanical actuators using polyaniline films," Synthetic Metals, vol. 71, no. 1-3, pp. 2211–2212, 1995.

[6]- D. W. Madden, "Conducting polymer actuators," PhD thesis, MIT, 2000.

[7]- S. S. Ge, T. H. Lee and C. J. Harris, *Adaptive Neural Networks Control of Robotic Manipulators*, World Scientific Publishing, 1998.

[8] G. Wallace, G. Spinks, "Conducting polymers–bridging the bionic interface", Soft Matter, vol .3, pp.665 – 671,2007.

[9]Yang Fang et al, "A scalable model for trilayer conjugated polymer actuators and its experimental validation", Materials Science and Engineering, vol. 28, pp.421–428, 2008.

[10] T. F. Otero and J. M. Sansinena, "Bilayer dimensions and movement inartificial muscles," Bioelectrochemistry and Bioenergetics, vol. 42, no. 2, pp. 117–122, 1997

[11] P. G. A. Madden, "Development and modeling of conducting polymer actuators and the fabrication of a conducting polymer based feedback loop", PhD thesis, Massachusetts Institute of Technology, 2003.

[12] B. Golubev and I. M. Horowitz, "Plant Rational Transfer function Approximation from Input-Output Data", International Journal of Control , Vol. 36,No. 4, pp. 711-723,1982.

[13] D.L. Boxall, R.A. Osteryoung, Journal of The Electrochemical Society 151 (2) E41, 2004.

[14] I. M. Horowitz. *Synthesis of Feedback Systems*, Academic Press, 1963.

[15] I. M. Horowitz and M. Sidi. "Synthesis of feedback systems with large plant ignorance for prescribed time domain tolerances". Int. J. Control, 16:287-309, 1972

[16] I. M. Horowitz and M. Sidi. "Optimum synthesis of nonminimum phase feedback system with plant uncertainty". Int. J. Control, 27:361-386, 1978.

[17] I. M. Horowitz. *Quantitative Feedback Design Theory (QFT),* volume 1. QFT Publications, 4470 Grinnel Ave., Boulder, Colorado 80303, USA, 1992.

[18] C.H. Houpis. *Quantitative Feedback Theory (QFT) For the Engineer: A Paradigm for the Design of Control Systems for Uncertain Nonlinear Plants.* Wright Laboratory, 1995.

[19]- Yaniv O., *Quantitative Feedback Design of linear and non-linear control systems*, Kluwer Academic Publication, Norwell, Massachussets, 1998.